ACS OMEGA

Article

AICAR Stimulates the Pluripotency Transcriptional Complex in Embryonic Stem Cells Mediated by PI3K, GSK3β, and β-Catenin

Gonzalo Alba,* Raquel Martínez, Fátima Postigo-Corrales, Soledad López, Consuelo Santa-María, Juan Jiménez, Gladys M. Cahuana, Bernat Soria, Francisco J. Bedoya, and Juan R. Tejedo
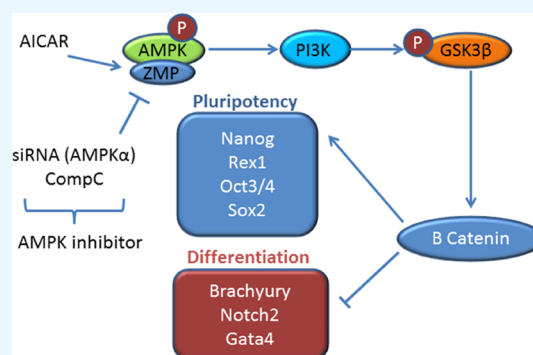
Read Online

ACCESS | Metrics & More | Article Recommendations

ABSTRACT: Pluripotent stem cells maintain the property of self-renewal and differentiate into all cell types under clear environments. Though the gene regulatory mechanism for pluripotency has been investigated in recent years, it is still not completely understood. Here, we show several signaling pathways involved in the maintenance of pluripotency. To investigate whether AMPK is involved in maintaining the pluripotency in mouse embryonic stem cells (mESCs) and elucidating the possible molecular mechanisms, implicated D3 and R1/E mESC lines were used in this study. Cells were cultured in the absence or presence of LIF and treated with 1 mM and 0.5 mM 5-aminoimidazole-4-carboxamide-1-β-D-ribofuranoside (AICAR), 2 mM metformin, compound C, and the PI3K inhibitor LY294002 for 24, 72, and 120 h. The levels of Nanog, Oct3/4, and REX1 and Brachyury, Notch2, and Gata4 mRNAs and Nanog or OCT3/4 protein levels were analyzed. Alkaline phosphatase and the cellular cycle were determined. The pGSK3β, GSK3β, p-β-catenin, and β-catenin protein levels were also investigated. We found that AMPK activators such as AICAR and metformin increase mRNA expression of pluripotency markers and decrease mRNA expression of differentiation markers in R1/E and D3 ES cells. AICAR increases phosphatase activity and arrests the cellular cycle in the G1 phase in these cells. We describe that AICAR effects were mediated by AMPK activation using a chemical inhibitor or by silencing this gene. AICAR effects were also mediated by PI3K, GSK3β, and β-catenin in R1/E ES cells. According to our findings, we provide a mechanism by which AICAR increases and maintains a pluripotency state through enhanced Nanog expression, involving AMPK/PI3K and p-GSK3β Ser21/9 pathways backing up the AICAR function as a potential target for this drug controlling pluripotency. The highlights of this study are that AICAR (5-aminoimidazole-4-carboxamied-1-b-riboside), an AMP protein kinase (AMPK) activator, blocks the ESC differentiation and AMPK is a key enzyme for pluripotency and shows valuable data to clarify the molecular pluripotency mechanism.

INTRODUCTION

Embryonic stem cell (ESC) lines are derived from the inner cell mass of embryonic blastocysts.[1−3] These cell lines have the ability to self-renew in vitro and differentiate into the three germ layers, a feature referred to as pluripotency.[4] The maintenance of pluripotency is controlled by the combined action of extrinsic factors such as leukemia inhibitory factor (LIF) and a network of signaling pathways and transcription factors.[5,6] Understanding the mechanisms of maintaining an undifferentiated state of embryonic cells is not only fundamentally important, but it is also critical for the development of approaches to the therapeutic use of pluripotent cells.

Nanog, Oct4, and Sox2 are key regulators of self-renewal in ESCs.[5,7−9] Expression of these genes gradually decreases during cell differentiation, whereas the expression of differentiation genes such as Brachyury, Notch2, and Gata4 augments.[10−13] Nanog confers pluripotency even in the absence of LIF, thus suggesting that this factor is a master regulator of ESC identity.[14,15] Furthermore, Nanog protein levels have been shown to be heterogeneous in a ESC population, thus suggesting that a Nanog "high" state is associated with pluripotency and self-renewal, while a Nanog "low" state leads to differentiation.[16] Nanog promotes the undifferentiated state by gene repression such as Gata4 and gene activation necessary for pluripotency such as Rex1.[4,17,18]

Adenosine monophosphate-activated protein kinase (AMPK), a serine/threonine protein kinase, which is activated by increased intracellular AMP or AMP/ATP (adenosine
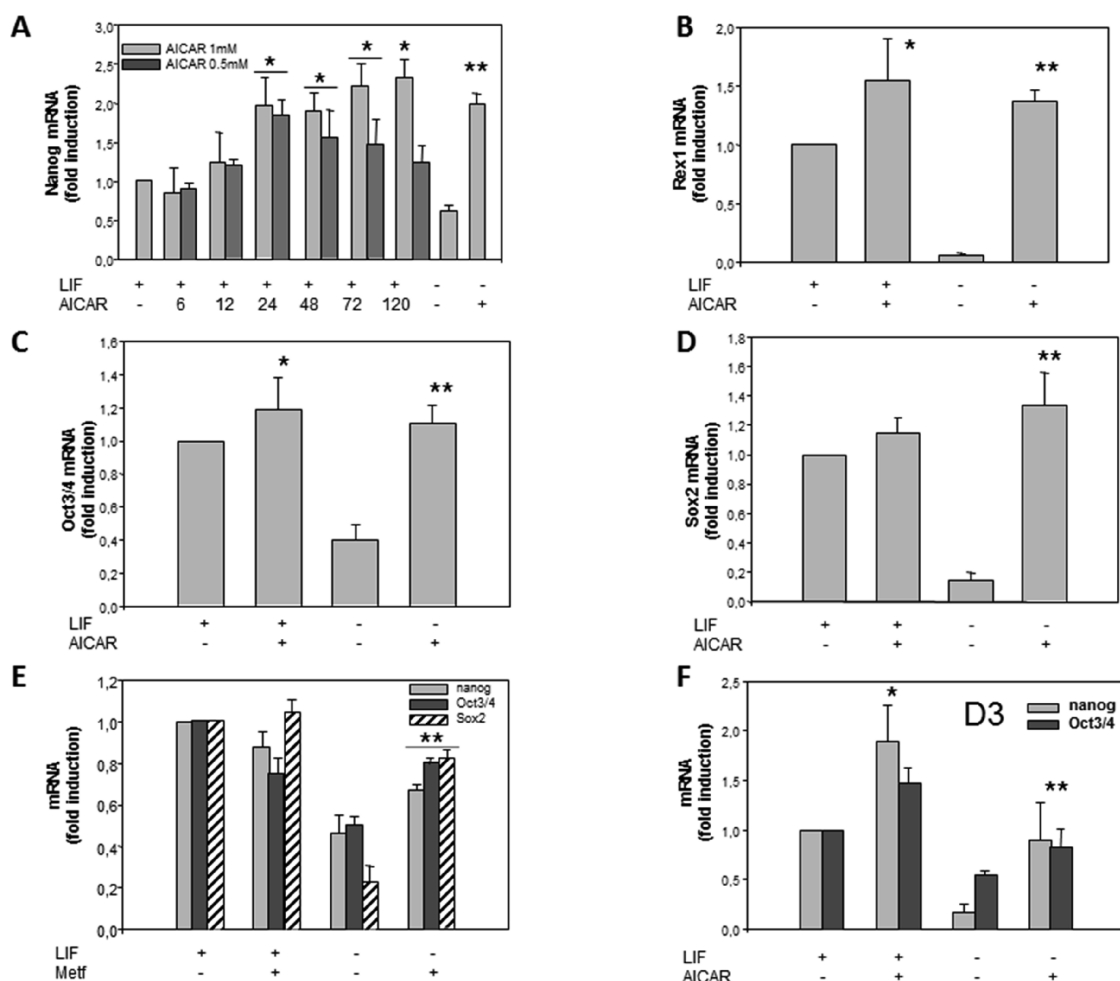
Figure 1. AICAR increases expression of pluripotency markers in R1/E and D3 ES cells. Cells were cultured with or without (A) 0.5 mM or (A, B, C, D, and F) 1 mM AICAR or (E) 2 mM metformin for 120 h or the indicated time (A) in the presence or absence of 1000 U/mL LIF. The levels of Nanog, Rex1, Oct3/4, and Sox2 mRNAs were analyzed by real-time RT-PCR, corrected for differences in β-actin mRNA levels (as endogenous gene), and expressed as fold induction. Values are plotted as the mean ± SEM ($n = 4$). Statistical significance: *$p < 0.01$ for AICAR- or metformin- and LIF-treated versus LIF-treated; **$p < 0.01$ for AICAR- or metformin-treated and LIF untreated versus LIF untreated.

triphosphate) ratio, plays an important role in mediating cellular energy homeostasis. Given the role of metabolic plasticity to enable stem cells to match the energetic demands of stemness and lineage specification, the function of AMPK as a hub to integrate metabolism, cell signaling, and transcriptional regulation in ESCs is extraordinarily essential. AMPK activation connects the response to metabolic stress and signaling pathways that induce cell cycle arrest, apoptosis, and differentiation, regulating the activity of different proteins.[19] However, the mechanisms by which AMPK affects self-renewal and pluripotency in ESCs remain unclear.[20−22]

With regard to the signaling pathways involved in the control of stemness, the phosphatidylinositol 3-kinase (PI3K)/ Akt pathway regulates both proliferation and pluripotency of mouse ESCs, partly due to its ability to sustain Nanog expression.[23−25] A target of Akt in a variety of cell systems is glycogen synthase kinase-3 (GSK-3); this serine/threonine kinase is involved in the regulation of the metabolism, proliferation, and differentiation during embryo development.[26] GSK3β inhibition by the PI3K /Akt system plays a prominent role in up-regulation of key master genes of pluripotency such as Nanog, c-Myc, and Tbx3.[27] PI3K

activation promotes self-renewal of ESCs partly due to GSK3β inhibition.

In the present study, we investigated the effects of 5-aminoimidazole-4-carboxyamide ribonucleoside (AICAR), an AMPK activator, on self-renewal and differentiation of mouse ESCs (mESCs). We found that AMPK activated by AICAR promotes the stemness state in mESCs in a process dependent on the PI3K/GSK3β regulation of Nanog expression. These results suggest that metabolic energy control systems are closely coupled to cellular growth and differentiation fates of ESCs and would be important evidence to further elucidate the molecular machinery of pluripotency.

■ RESULTS

AICAR and Metformin Increase mRNA Expression of Pluripotency Markers in R1/E and D3 ES Cells. Nanog is a pluripotent cell marker that is highly expressed in mESC cells.[28,29] We have performed RT-PCR at different times to know the time needed to increase AICAR-induced Nanog expression in these cells (Figure 1A).The treatment with 1 mM AICAR for 6, 12, 24, 48, 72, and 120 h in the presence of LIF progressively and significantly increases the expression between 24 and 120 h. Meanwhile, at a concentration of 0.5 mM
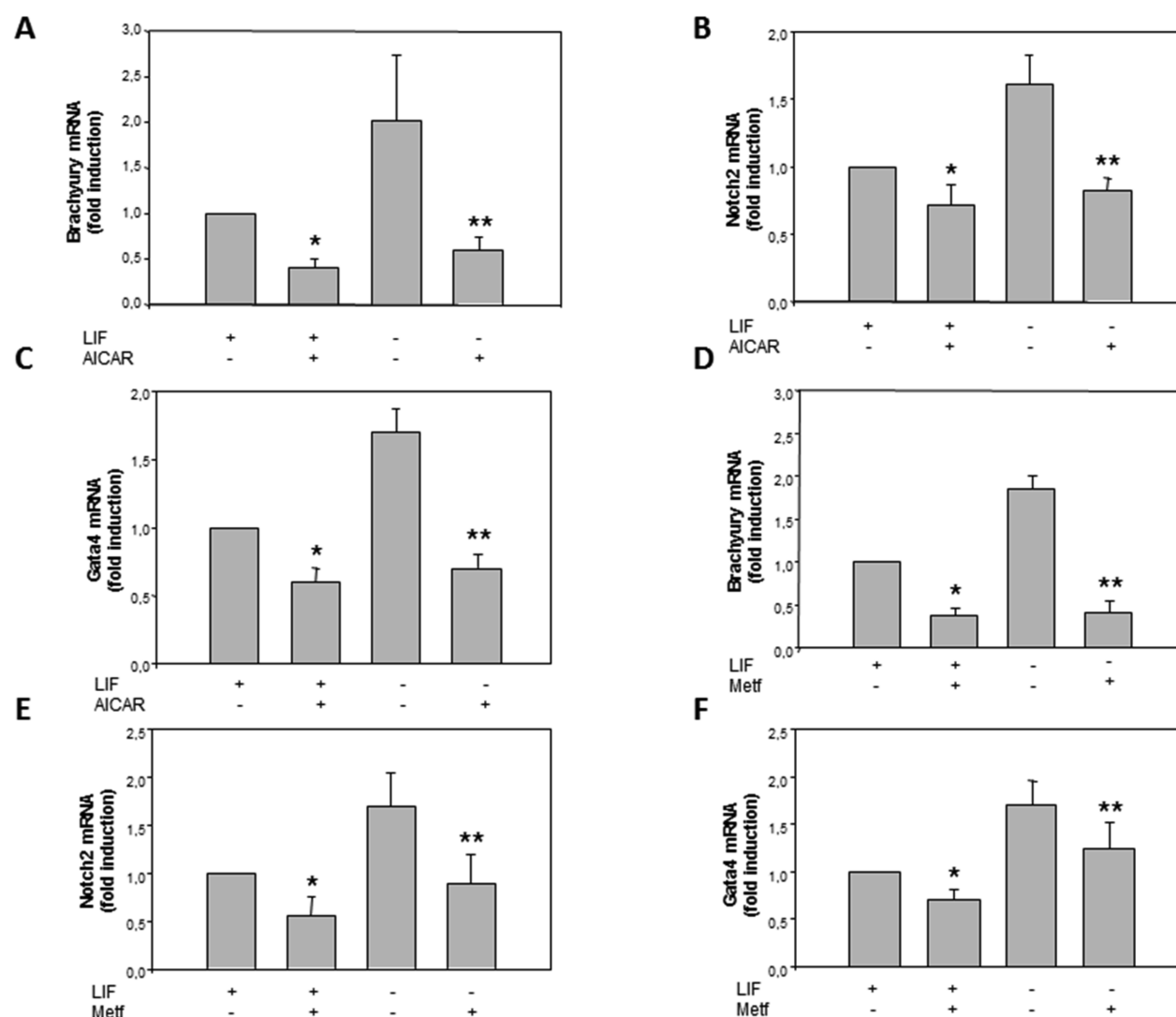
Figure 2. AICAR decreases expression of differentiation markers in R1/E ES cells. Cells were cultured with or without (A−C) 1 mM AICAR or (D−F) 2 mM metformin for 120 h in the presence or absence of 1000 U/mL LIF. The levels of Brachyury, Notch2, and Gata4 mRNAs were analyzed by real-time RT-PCR, corrected for differences in β-actin mRNA levels (as endogenous gene), and expressed as fold induction. Values are plotted as the mean ± SEM ($n = 4$). Statistical significance: *$p < 0.01$ for AICAR- or metformin- and LIF-treated versus LIF-treated; **$p < 0.01$ for AICAR- or metformin-treated and LIF untreated versus LIF untreated.

AICAR, the highest increase is at 24 h and then decrease between 48 and 72 h, although they were significantly higher than the control in the presence of LIF. According to these results, we usually selected a time of 120 h and 1 mM AICAR to carry out our assays and study the different markers.

To determine whether LIF treatment modifies the effects of AICAR on Nanog expression, Nanog levels were studied in the absence of LIF. It was observed that, in cells cultured in the absence of LIF, the expression of Nanog decreased significantly; under these conditions, the treatment with AICAR cancels the effect of LIF withdrawal (Figure 1A).

Next, we asked whether levels of other pluripotent stem cell markers were also altered by AICAR treatment. Rex1, Oct3/4, and Sox2 are transcription factors essential in maintaining the pluripotency and self-renewal and are highly expressed in ES cells.[5,7−9] In our study, we observed that, in LIF presence, AICAR treatment induced a clear increase in Rex1 (Figure 1B) but did not induce a significant increase in Oct3/4 (Figure 1C) and Sox2 (Figure 1D). However, the treatment with AICAR in the absence of LIF significantly increased the expression levels

of Rex1 (Figure 1B), Oct3/4 (Figure 1C), and Sox2 (Figure 1D). However, synergistic or additive effects were not observed in any pluripotency genes in LIF + AICAR treatment in combinational treatments.

To test whether other AMPK activators had an effect on pluripotency markers in R1/E stem cells, treatment with 2 mM metformin was analyzed. Figure 1E shows that there were no significant changes in Nanog, Oct3/4, and Sox2 mRNA expressions with metformin treatment in LIF presence. However, significant increases were observed in these genes in the absence of LIF. Nanog increased by 2.3-fold, Oct3/4 by 1.5−fold, and Sox2 by 3-fold (Figure 1E).

To study if this effect occurs in other cell types, mouse embryonic stem D3s (ES-D3) were stimulated with 1 mM AICAR for 120 h (Figure 1F). The Nanog mRNA levels were detected by quantitative RT-PCR, which showed a significant increase in the presence of LIF (1.8 fold change) and the absence of LIF (11.9 fold change). In addition, mRNA levels of other pluripotency marker such as Oct3/4 significantly
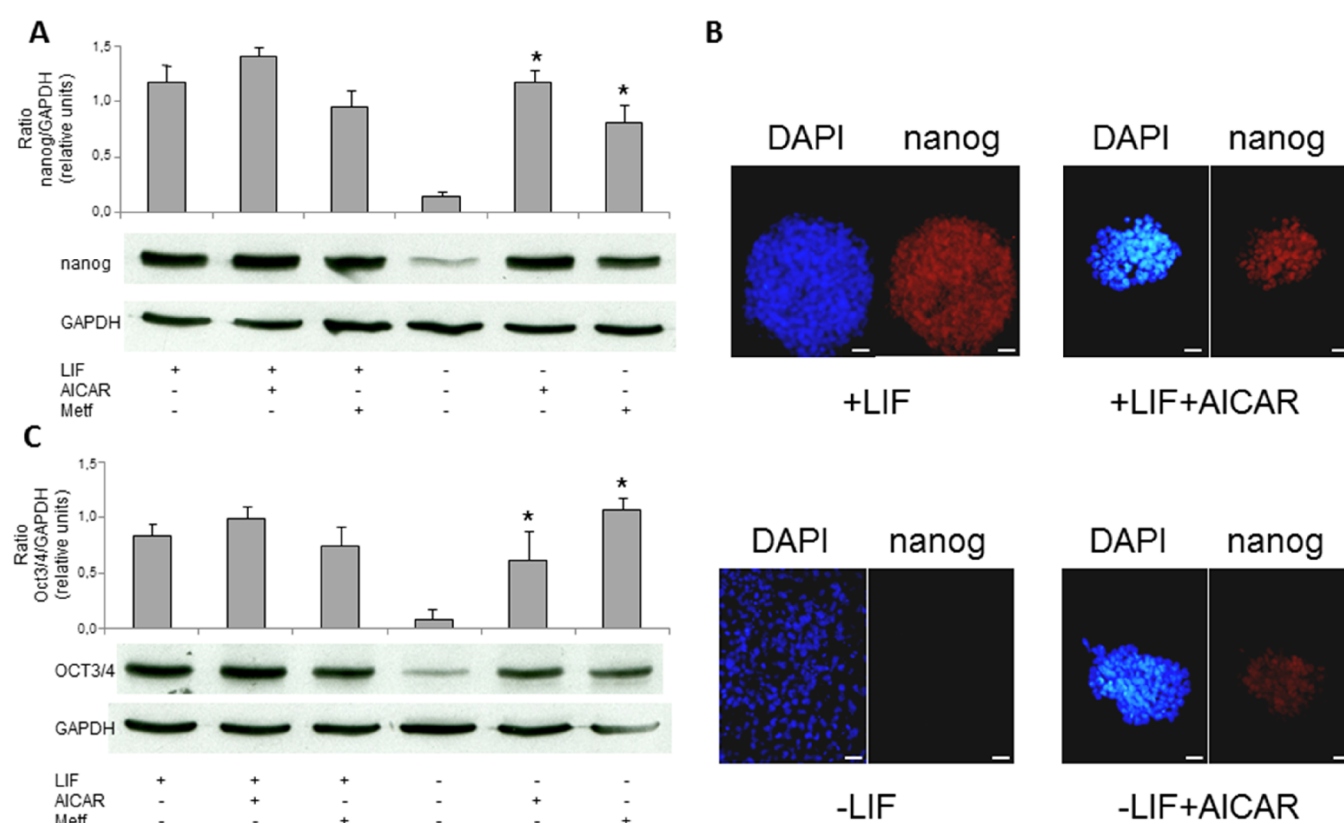
Figure 3. AICAR increases protein expression of pluripotency markers in R1/E ES cells. Cells were cultured with or without (A−C) 1 mM AICAR or (A and C) 2 mM metformin for 120 h in the presence or absence of 1000 U/mL LIF. Nanog or OCT3/4 protein levels were analyzed on cell lysates by western blotting (A and C) or by immunocytochemistry. Scale bars = 25 μm (B) and expressed as arbitrary units. GAPDH bands are shown for the sake of loading controls (A and C). Control cells were cultured for the same time without any additions. The panel is representative of a set of four experiments yielding similar results, and values are plotted as the mean ± SEM ($n = 4$). *$p < 0.01$ for AICAR- or metformin-treated versus control.

increased under these conditions with a fold change of 1.5 (Figure 1F).

AICAR and Metformin Decrease mRNA Expression of Differentiation Markers in R1/E ES Cells. In order to determine whether the effect of AICAR, while increasing the expression of pluripotency genes, decreases the expression of early differentiation marker genes, we analyzed the expression of Brachyury, Notch2, and Gata4.[28,29] Treatment with 1 mM of AICAR for 120 h in the presence of LIF significantly decreases the mRNA expression of Brachyury, Notch2, and Gata4 with fold changes of 0.6, 0.3, and 0.4 (Figure 2A−C), respectively. In the absence of LIF, these genes decreased with fold changes of 0.65, 0.55, and 0.6, respectively. These results indicate that AICAR significantly decreases differentiation markers, thus implicating its role in the pluripotency of mESC. However, synergistic or additive effects were not observed in differentiation genes in LIF + AICAR treatment in combinational treatments.

Similar results were detected in metformin treatment, mRNA levels of the differentiation markers Brachyury (Figure 2D), Notch2 (Figure 2E), and Gata4 (Figure 2F) significantly decreased with fold changes of 0.55, 0.45, and 0.2, respectively, in R1/E stem cells treated with 2 mM metformin in the absence of LIF for 120 h and 0.62, 0.5, and 0, respectively, in the presence of LIF. As expected, similar results were observed in the AICAR or metformin treated cells, both AMPK activators in R1/E for pluripotency and differentiation markers.

This shows that activation of AMPK by AICAR or metformin is implicated in pluripotency and differentiation in mESC.

AICAR Increases Protein Expression of Pluripotency Markers in R1/E ES Cells. Following the experiments, we sought to determine if changes in mRNA expression, as described above, correspond to changes in protein expression. Thus, we studied the effect of AMPK activators (AICAR and metformin) on the expression of pluripotency markers proteins (Nanog and Oct3/4). Western blot analysis showed an increased level of Nanog in R1/E treated with 1 mM AICAR or 2 mM metformin in the absence of LIF with fold changes of 8 and 5, respectively (Figure 3A). Subsequent experiments using confocal microscopy immunofluorescence analyses were performed in R1/E stem cells treated with 1 mM AICAR for 120 h in the presence and absence of LIF (Figure 3B). Results show Nanog marker expression in treated cells with AICAR and LIF compared to AICAR untreated cells in the presence of LIF. In the absence of LIF, a stronger increment of Nanog marker expression was observed in treated cells with AICAR. Similar results were detected in Oct3/4 protein expression by western blot analysis (Figure 3C), reinforcing the role of AICAR in pluripotency.

AICAR Increases Phosphatase Activity and Arrests Cellular Cycle in the G1 Phase in R1/E ES Cells. The measure of alkaline phosphatase enzymatic activity is also a pluripotency indicator in embryonic stem cells.[30] Optical microscopy analyses were performed in R1/E ES cells cultured with 1 mM AICAR in the presence or absence of 1000 U/mL
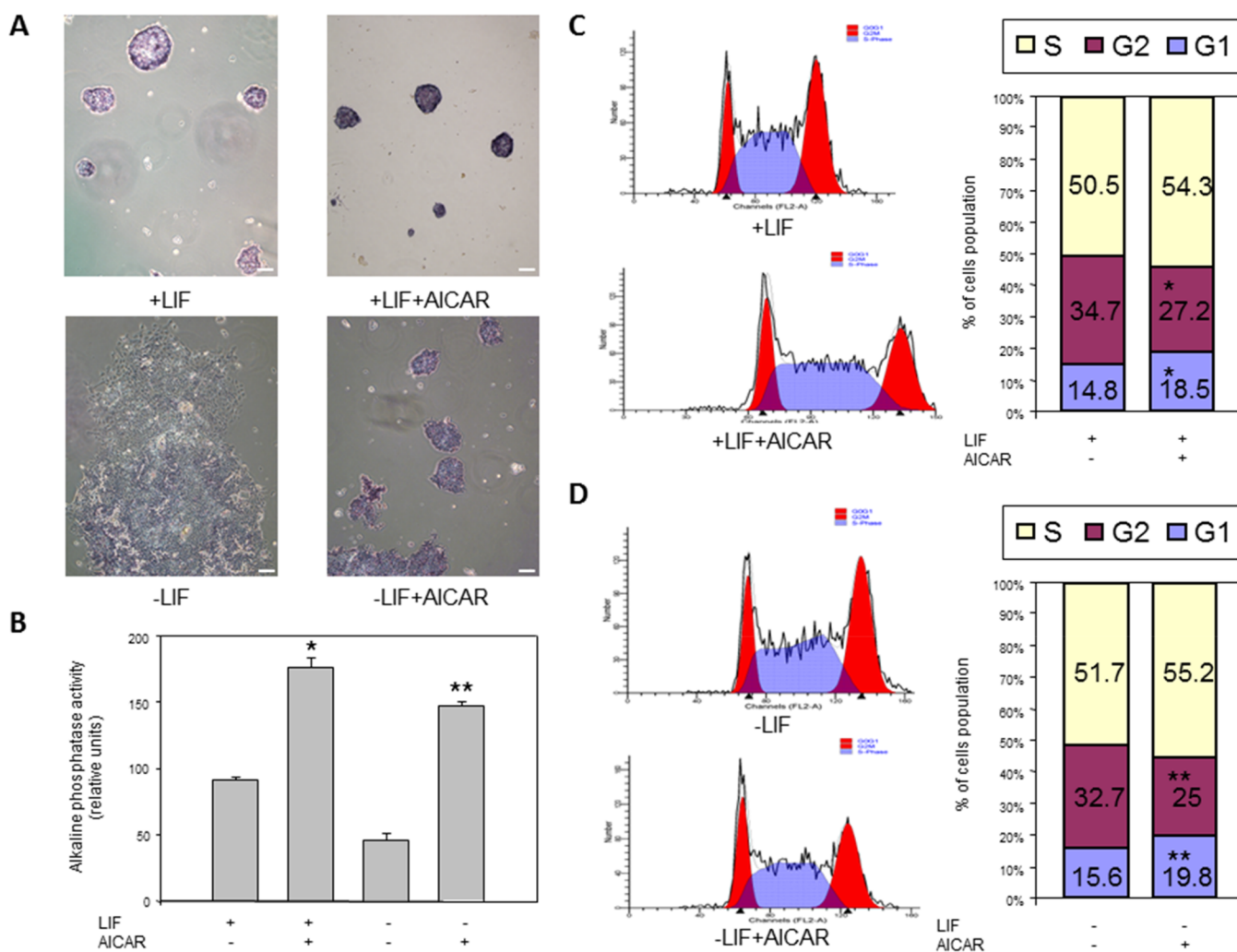
Figure 4. AICAR increases phosphatase activity and G1 phase R1/E ES cells. Cells were cultured with or without 1 mM AICAR for 120 h in the presence or absence of 1000 U/mL LIF. Alkaline phosphatase staining was performed and observed by a microscope. Scale bars = 200 μm (A), and values are plotted as the mean ± SEM of intensity quantification ($n = 4$) (B). Control cells were cultured for the same time without any additions. The cellular cycle was analyzed by a flow cytometer (C and D, left). Bar charts correspond to the percentage of cells in different cell cycle phases (C and D, right). The panel is representative of a set of four experiments yielding similar results, and values are plotted as the mean ± SEM ($n = 4$). Statistical significance: *$p < 0.01$ for AICAR- and LIF-treated versus LIF-treated. **$p < 0.01$ for AICAR-treated LIF untreated versus LIF untreated.

LIF for 120 h when investigating the effects of AICAR on alkaline phosphatase activity. In the presence of LIF with 1 mM AICAR, cells showed an increased positive alkaline phosphatase activity when compared to the control group (Figure 4A,B), suggesting a role of AICAR in pluripotency. We obtained 2-fold more of alkaline phosphatase activity in cells treated with AICAR compared to untreated cells in the presence of LIF. However, cells showed differentiation in the absence of LIF, and when 1 mM AICAR was supplemented, a 3-fold higher activity was observed in alkaline phosphatase. However, we observed that AICAR treatment induced colonies compaction, and this further increased the intense signal. Moreover, we also investigated the effects of 0.5 mM AICAR in cells cultured with 1000 U/mL LIF for 24 h on alkaline phosphatase activity. A positive alkaline phosphatase activity was shown when cells were treated with 0.5 mM AICAR in the presence of LIF (data not shown). We obtained 0.3-fold more of alkaline phosphatase activity in cells treated with AICAR when compared to untreated cells.

In most cases, cell response to the emergence of energy deficiency is accompanied by cell cycle arrest.[31] We analyzed the mESC cell cycle distribution by a flow cytometry method and found that AICAR treatment in mESCs dramatically decreased the G2 phase cell population but increased that of the G1 phase (Figures 4C and 4D), suggesting a slowing down of the proliferation rates after AICAR treatment.

AICAR Effects Are Mediated by AMPK Activation in R1/E ES Cells. To determine whether AICAR activates AMPK, R1/E cells were treated with 1 mM AICAR for 30 min in the presence or absence of LIF. Figure 5A shows that the enzyme was not phosphorylated under basal conditions and its activation was induced following exposure to AICAR by western blot with anti-AMPK-P, having fold changes of 10 and 5 in the presence and absence of LIF, respectively.

To determine whether the effect of AICAR in pluripotency was mediated through an AMPK pathway, we analyzed the expression of Nanog and Rex1 by using compound C, a specific AMPK inhibitor. R1/E cells were pre-incubated for 30 min with or without 2.5 μM compound C and incubated with
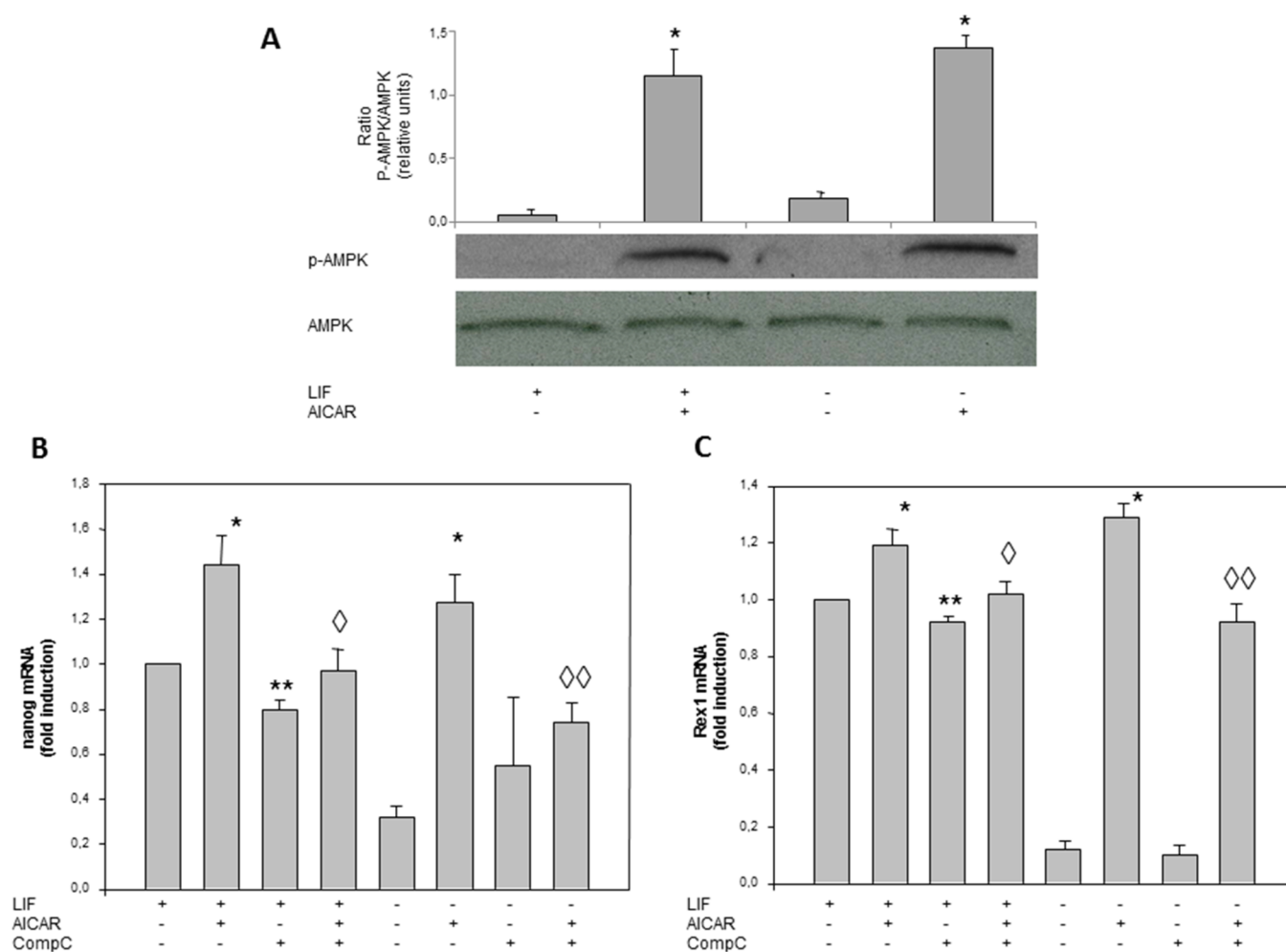
Figure 5. AICAR effects are mediated by AMPK activation in R1/E ES cells. Cells were cultured with or without (A−C) 1 mM AICAR and (B, C) 2.5 μM compound C for 120 h in the presence or absence of 1000 U/mL LIF. p-AMPK and AMPK protein levels were analyzed on cell lysates by western blotting and are given in arbitrary units. GAPDH bands are shown for the sake of loading controls (A). Control cells were cultured for the same time without any additions. The panel is representative of a set of four experiments yielding similar results, and values are plotted as the mean ± SEM (n = 4). The Nanog levels and Rex1 mRNAs were analyzed by real-time RT-PCR, corrected for differences in β-actin mRNA levels (as endogenous gene), and expressed as fold induction, and values are plotted as the mean ± SEM (n = 4) (B and C). Statistical significance: *p < 0.01 for AICAR- and LIF-treated or -untreated versus LIF-treated or -untreated; **p < 0.01 for compound C and LIF-treated versus LIF treated; ◊p < 0.05 for compound C- AICAR- and LIF treated versus AICAR- and LIF-treated; ◊◊p < 0.05 for compound C- and AICAR-treated versus AICAR-treated.

1 mM AICAR for 120 h (Figure 5B,C). A significant increase in Nanog mRNA expression levels in the absence of LIF was shown with AICAR treatment with a fold change of 9.5 (Figure 5B). In the presence of AICAR and compound C, we observed that compound C partially reduced Nanog mRNA expression levels with a fold change of 0.6 (Figure 5B), involving AMPK in Nanog expression. There were no significant differences (Figure 5B) when compound C was added to the medium in the absence of LIF. Doses higher than 2.5 μM of compound C were toxic for R1/E cells. Similar results were detected in Rex1 expression (Figure 5C), although the Rex1 expression was more stimulated by AICAR treatment and the compound C effect was lesser.

Transfection with Specific AMPKα1 siRNA Decreased AICAR-Stimulated Pluripotent Genes mRNA Expression in R1/E Cells. The alternative trial methodology to inhibit AMPK was the use of small interference RNA (siRNA) against both α1 and α2 isoforms of the catalytic subunits of the enzyme. Transfection with AMPK α2siRNA inhibits AMPKα2

but not AMPKα1 (Figure 6A,B). In Figure 6C, we observed that AMPKα2 siRNA transfection partially reverted the AICAR-stimulated Nanog expression in the presence or absence of LIF. Similar results were detected in Rex1 expression (Figure 6D).

AICAR Effects Were Mediated by PI3K, GSK3β, and β-catenin in R1/E ES Cells. To determine whether the effect of AICAR in pluripotency was mediated through the PI3K pathway, the Nanog expression was analyzed using LY294002, a pharmacological inhibitor of PI3K in R1/E cells. R1/E cells were pre-incubated for 30 min with or without 20 μM of LY294002 and incubated with 1 mM AICAR for 120 h in the absence of LIF (Figure 7A). AICAR treatment increased Nanog mRNA expression, in the absence of LIF, 2.75 times. When LY294002 was added alone, no significant difference was observed. LY294002 treatment reverted the AICAR effect on Nanog mRNA expression. These results indicate that PI3K signaling is involved in the expression of Nanog mRNA levels by means of AICAR.
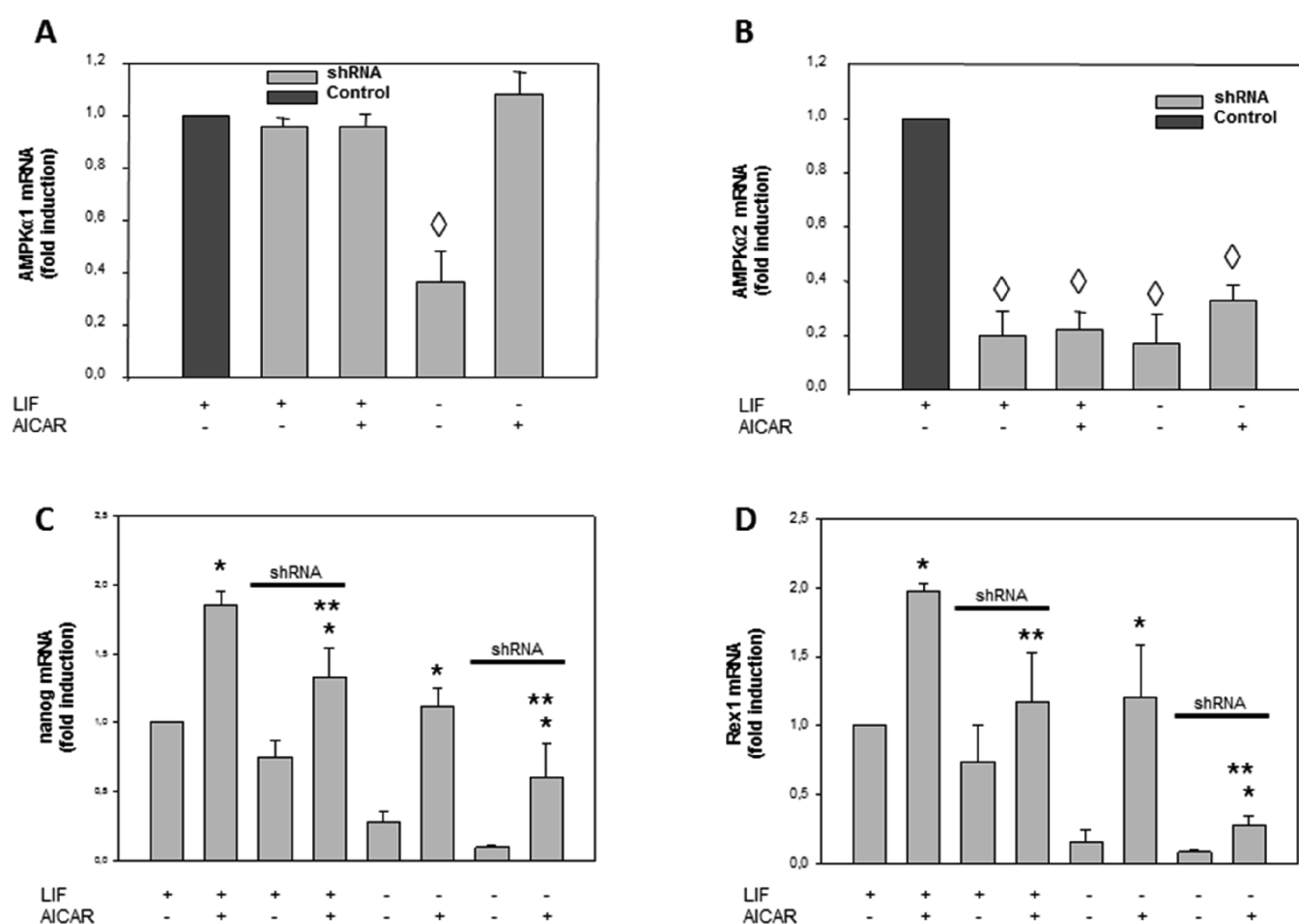
Figure 6. AICAR effects are mediated by AMPK activation in R1/E ES cells. Cells were transfected with shRNA AMPKα2 or shRNA control and cultured with or without 1 mM AICAR for 120 h in the presence or absence of 1000 U/mL LIF (A−D). Levels of AMPKα1, AMPKα2, Nanog, and Rex1 mRNAs were analyzed by real-time RT-PCR, corrected for differences in β-actin mRNA levels (as endogenous gene), and expressed as fold induction. Values are plotted as the mean ± SEM ($n = 4$). Statistical significance: *$p < 0.01$ for AICAR-treated versus AICAR-untreated; **$p < 0.01$ for AICAR- and shRNA AMPKα2-treated versus AICAR-treated; ◊$p < 0.01$ for shRNA AMPKα2-treated versus shRNA AMPKα2-untreated.

To examine the functional role of GSK3β in pluripotency, the p-GSK3β Ser21/9 protein levels have been analyzed in cells treated with AICAR and LY294002 (Figure 7B). Cells were pre-incubated for 30 min with or without 20 μM of inhibitor LY294002 and incubated in the absence of LIF with 1 mM AICAR for 24 h. As seen in Figure 7B, a significant increase in p-GSK3β Ser21/9 in the absence of LIF was shown with AICAR treatment with a fold change of 2.6. When only LY294002 was added to the medium, in the absence of LIF, there were no significant differences versus the control. In the presence of AICAR and LY294002, a total reversion was observed. LY294002 was seen to reduce the activator effect of AICAR on p-GSK3β Ser21/9 protein levels in the absence of LIF, indicating that p-GSK3β Ser21/9 signaling is involved in an undifferentiated state through AICAR.

A key GSK-3 substrate is β-catenin, and Wnt/β-catenin signaling pathway is essential for gene transcriptional regulation of mESCs, including pluripotency genes.[32] For this reason, the effect of AICAR and metformin treatment on β-catenin was tested. Figure 7C shows that both treatments induced a clear increase in both the presence and absence of LIF.

In agreement with these findings, the effect of AICAR on Nanog could be regulated through AMPK/PI3K pathways in mouse embryonic stem cells.

■ DISCUSSION

AICAR and metformin, common AMPK activators, participate in pathways that include BMP, MAPK, and TGF-β signaling, which are associated with self-renewal and differentiation.[33] Furthermore, AICAR is involved through the epigenetic modifications in maintaining pluripotency.[33] In this study, we present one mechanism by which AICAR regulates Nanog expression in mESCs. Several studies have shown that AICAR maintains J1 mESC self-renewal and pluripotency by regulating transcription factors, increasing the expression of pluripotency markers such as Nanog, Oct4, and Sox2.[21] Conversely, AICAR has been described to decrease Nanog expression in mESCs, differentiated mESCs to embryonic bodies (EBs) in serum, suggesting a decrease in Nanog expression in this state.[34] Other authors described a decrease in Nanog expression from 72 to 168 h in differentiated embryonic body cells when compared to undifferentiated ES cells.[35] To explain this discrepancy, our study is based on the AICAR effect on Nanog expression in undifferentiated cells to embryonic body cells.
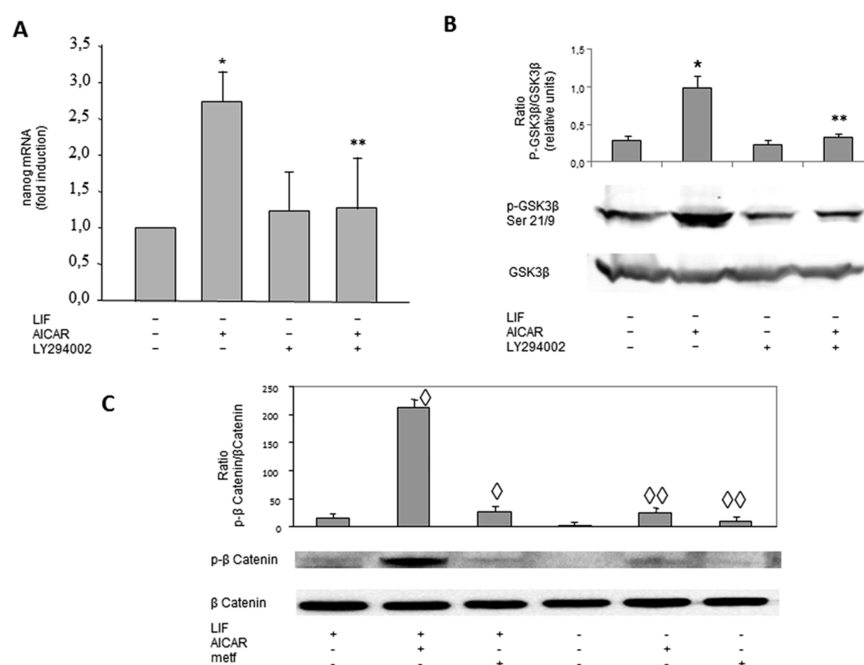
Figure 7. AICAR effects are mediated by PI3K, GSK3β, and β-catenin in R1/E ES cells. Cells were cultured with or without (A, B) 20 μM LY294002 for 30 min previously to treatment with (A−C) 1 mM AICAR or (C) 2 mM metformin for 120 h in the presence or absence of 1000 U/mL LIF. The levels of Nanog mRNAs were analyzed by real-time RT-PCR, corrected for differences in β-actin mRNA levels (as endogenous gene), and expressed as fold induction (A). pGSK3β, GSK3β, p-βcatenin, β-catenin, and β-actin protein levels were analyzed on cell lysates by western blotting and are given in arbitrary units. Control cells were cultured for the same time without any additions. The panel is representative of a set of four experiments yielding similar results, and values are plotted as the mean ± SEM ($n = 4$). Statistical significance: *$p < 0.01$ for AICAR-treated versus control; **$p < 0.01$ for LY294002- and AICAR-treated versus AICAR-treated; $\Diamond p < 0.05$ for AICAR- or metformin- and LIF treated versus LIF-treated; $\Diamond\Diamond p < 0.05$ for AICAR- or metformin-treated and LIF untreated versus LIF untreated.

We present a kinetic with different doses of AICAR on Nanog expression, which demonstrates that AICAR treatment increases Nanog expression in mESCs, previously not shown in studies. Similarly, AICAR sustains pluripotency in J1 mouse embryonic stem cells.[36] To further confirm whether our findings may also be applicable to other different lines of R1/E, we tested AICAR treatment for D3 cell lines, obtaining an increment in Nanog expression.

The present data shows that AICAR up-regulates Nanog and Oct4 in mESCs as found by others,[33] and furthermore, we verify that other pluripotency markers, such as Rex1, are also up-regulated by AICAR. Although AICAR is the most common AMPK activator, we also tested whether other activators such as metformin are sufficient for maintaining pluripotency. Recently, metformin has been reported to decrease Nanog expression via the JNK pathway in HepG2 cells.[37]

Besides, the expression of some differentiation markers, such as Brachyury, Notch2, and Gata4, are down-regulations in R1/E cells. In addition, expression of another pluripotency marker such as Oct3/4 and differentiation markers such as Brachyury, Notch2, and Gata4 were stimulated and inhibited respectively in the absence of LIF after treatment with metformin.[37]

In spite of this difference being of a cellular type, our study supports that metformin induces a significant increment in pluripotency in mESCs. These results suggest that metformin, an AMPK activator, contributes to an undifferentiated state in mESCs. In agreement with our findings, AMPK activators increase Nanog expression in mESCs. However, our results show up-regulation of the Nanog expression for RNA and protein levels in mESCs.

Alkaline phosphatase is a hydrolase enzyme responsible for dephosphorylating molecules such as nucleotides and proteins under alkaline conditions. Alkaline phosphatase is a universal pluripotency marker for all types of pluripotent stem cells including embryonic stem cells, embryonic germ cells, and induced pluripotent stem cells. A low level of alkaline phosphatase activity denotes the restriction of pluripotency and differentiation. It has been suggested that this increase is related to an intense substrate dephosphorylation associated with the rapidly proliferating metabolism of ES cells. Andäng et al.[38] suggest the importance of GABA synthesis in ES cells for the regulation of their proliferation and self-renewal and that alkaline phosphatase participates in GABA synthesis. Our results show a significant increase in alkaline phosphatase activity after AICAR treatment in R1/E ES cells that correlates well with the effects found in the previous pluripotent markers described.

The exact mechanism by which AICAR treatment controls mESC pluripotency is still unclear. The present results provide one mechanism in which AICAR increases Nanog expression involving AMPK/PI3K in the maintenance of pluripotency. An initial step that contributes to explain this mechanism is its inhibition by compound C, AMPK inhibitors.[39] These data suggest that AMPK activation by AICAR regulating Nanog expression plays a role in the pluripotency for mESCs.

Next, experiments that silence RNA (siRNA) of the isoform α2 of the AMPK catalytic subunit were also performed to corroborate the findings observed with compound C. On inhibiting the catalytic ability of the AMPK enzyme, a partial reversion in Nanog mRNA expression was observed in cells treated with AICAR. Similar results were found in Rex1

expression. In conclusion, these results may lead us to believe that AMPK is a key enzyme for pluripotency.

The role AMPK plays in stem cells is currently a topic of great interest. Recently resveratrol has been reported to enhance pluripotency in other mouse embryonic stem cells (IOUD2) by activating the AMPK/Ulk1 pathway and down-regulation of mammalian target of rapamycin complex 1 (mTORC1).[40] Lin et al.[41] described the 2,3,5,4′-tetrahydroxystilbene-2-O-β-glucoside potentiates self-renewal of human dental pulp stem cells via the AMPK/ERK/SIRT1 pathway. Moreover, Gong et al. found a critical role for AMPK-dependent phosphorylation of the ULK1 pathway in maintaining ESC self-renewal and pluripotency.[42]

PI3K signaling modulates Nanog expression, suggesting that PI3K plays an important role in regulating the networks of intrinsic factors that contribute to the determination of ES cell fate.[24] The activation of PI3K by AICAR may provide this signaling pathway as a potential target for this drug.[14] Treatment of ES cell cultures with only LY294002 did not alter Nanog expression. Interestingly, our results show a significant decrease in Nanog expression in the cells treated with AICAR and LY294002, thus suggesting that AICAR regulates Nanog expression through PI3K pathway in these cells.

Additionally, GSK3β, whose phosphorylation of serine 9 and/or serine 21, results in inactivation of the GSK3 kinases. Thus, high phosphorylation levels of these sites indicate lower activity of this kinase in mESCs.[43]

Inhibition of GSK-3 is said to enhance self-renewal of mouse ESC protein.[43] Consistent with this finding, we observed that AICAR treatment up-regulated phosphorylation of the inactive form GSK3β (Ser21/9), associated with the undifferentiated state. When AICAR is combined with LY294002, we observed down-regulated phosphorylation of GSK3β (Ser21/9), associated with a differentiated state. These results further support a correlation between GSK3β, AICAR-induced Nanog expression, and undifferentiated state.

A key GSK-3 substrate is β-catenin, the effector molecule of the Wnt/β-catenin signaling pathway, which acts as a transactivator of target genes through its interactions with TCF/LEF transcription factors. GSK-3-mediated phosphorylation of β-catenin results in its ubiquitination and proteasomal degradation.[44] β-catenin-mediated Wnt signaling is assumed to play a major role in embryonic stem cells in maintaining their stem cell character. Mouse embryonic stem cells (mESCs) devoid of GSK-3 display extremely high levels of signaling-competent β-catenin and have a profound block in their capacity to differentiate into cell types of the three germ lineages.[45] Raggioli et al.,[46] in genetically modified mouse embryonic stem cell lines, allow for the deletion of β-catenin in a controlled manner, demonstrating that β-catenin is vital for the integrity of mouse embryonic stem cells. Kelly et al.[47] show that β-catenin forms a complex and enhances the activity of Oct-4, a core component of the transcriptional network regulating pluripotency. Present studies show an increase in β-catenin after AICAR treatment in agreement with the results described to GSK3.

The differentiation in mESCs is generally associated with an increment in the G1 phase duration,[48,49] while the G1 phase shortens, and the S, G2/M phase increment is related to pluripotency.[50]

When we compared results in +LIF versus −LIF (this treatment is a differentiated condition, first column in panels C

and D in Figure 4), we observed that the G1 phase was slightly increased in a differentiation condition (from 14.8 to 15.6%) in concordance with that described before. However, it was surprising that, both in the presence and in the absence of LIF, the AICAR addition did the opposite, i.e., this treatment increased the cell number slightly but significantly in the G1 phase. Previously, similar results have been published in mESCs treated with 2i+LIF[51] and 2i+LIF+Serum;[52] in these, the authors observed that the G1 phase duration in pluripotency conditions is slightly but significantly greater than in differentiation conditions (2i is a GSK3β inhibitor that activates the Wnt/β-catenin pathway and this promoted pluripotency).[32]

The GSK3β phosphorylate in Ser (Ser21/9) increased in AICAR treatment, and this agrees with Wnt/β-catenin pathway activation and increases β-catenin phosphorylation in Tyr and pluripotency maintenance.[29] In conclusion, AICAR effects on the G1 phase duration and Nanog and Rex1 levels (panels B and C in Figure 5) agree with 2i effects (as described before) and other GSK3β inhibitors, such BIO and CHIR9902, which also promoted pluripotency.[53] The AICAR mechanism by which it increases G1 phase and promotes pluripotency should be studied in more detail.

We do not discard other possible pathways in which AICAR may affect Nanog expression, independently of AMPK.[37] In addition, AICAR induces differentiation of neural stem cells via activating the JAK/STAT3 pathway independently of AMPK.[54]

According to these findings, we provide a mechanism by which AICAR increases and maintains pluripotency through enhanced Nanog expression, involving AMPK/PI3K and p-GSK3β Ser21/9 pathways supporting the function of AICAR as a potential target for this drug controlling pluripotency.

■ EXPERIMENTAL SECTION

Cell Culture and Treatments. D3 and R1/E mESCs lines (ATTC, Manassas, USA) were cultured at a low density in Dulbecco's modified Eagle's medium (DMEM-Glutamax) (high glucose) (Gibco, Carlsbad, CA, USA) supplemented with 15% fetal bovine serum (FBS) (Hyclone, Logan, UT, USA), 1% non-essential amino acids (Gibco, Carlsbad, CA, USA), 0.1 mM 2-mercaptoethanol (Gibco, Carlsbad, CA, USA), 2 mM L-glutamine (Gibco, Carlsbad, CA, USA), 100 U/mL penicillin (Gibco, Carlsbad, CA, USA), and 0.1 mg/mL streptomycin (Gibco, Carlsbad, CA, USA). The culture was carried out at 37 °C under 5% CO_2. Undifferentiated state was maintained by adding 1.000 U/mL leukemia inhibitor factor (LIF) (Chemicon, Charlottesville, VA, USA) to the culture medium. For experiments with mESCs, 150 cells/cm² were cultured for 120 h in colonies in the absence or presence of LIF and treated with 1 and 0.5 mM 5-aminoimidazole-4-carboxamide-1-β-D-ribofuranoside (AICAR) (Toronto Research Chemicals Inc., Ontario, Canada), 2 mM metformin (METF) (Sigma, St. Louis, MO, USA), 2.5 μM compound C (COMP C) (Sigma, St. Louis, MO, USA), and 20 μM PI3K inhibitor LY294002 (Sigma) (Sigma, St. Louis, MO, USA) for 24, 72, and 120 h; the inhibitor was added 30 min before AICAR treatment.

RNA Isolation. Collected mESCs were washed with PBS, and Easy Blue reagent was used (Intron Biotechnology, Gyeonggi-do, Korea) following phenol/chloroform extraction. Total RNA was precipitated in 2-propanol, washed with ethanol, suspended in nuclease-free water and stored at −80

°C until use for cDNA synthesis. RNA concentration was measured in a NanoDrop ND-1000 Spectrophotometer (NanoDrop Technologies, Wilmington, USA).

Reverse Transcription and RT- PCR. cDNA synthesis was performed with 1 μg of total RNA using the SensiFAST cDNA Synthesis Kit (BIOLINE, London, United Kingdom) according to the manufacturer's instructions in a volume of 20 μL for 10 min at 25 °C, 15 min at 42 °C, 5 min at 85 °C and held to 4 °C. The cDNA obtained was diluted 1:2 and used as a template for quantitative PCR using SYBR Premix Ex Taq (Takara BIO Inc., Shiga, Japan). Each 20 μL reaction included 10 μL of SYBR Premix Ex Taq (2X), 0.4 μL of 10 μM primers, 0.4 μL of ROX Reference Dye II (50X), 1 μL of diluted cDNA, and water to a final reaction volume of 20 μL. cDNA levels were detected with an ABI Prism 7500 (Applied Biosystems, Foster City, CA, USA).

According to the following protocol: 95 °C X 10 min, 95 °C X 30 s, and 60 °C X 1 min for 40 cycles and data collection at 60 °C. Results were normalized with β-actin, and all the data were analyzed with the $2^{-\Delta\Delta Ct}$ method. The PCR primers forward (F) and reverse (R) used are as follows: Nanog F: AGCAGATGCAAGAACTCTCCTCCA; Nanog R: CCGCTTGCACTTCATCCTTTGGTT; Oct4 F: AGCTGCTGAAGCAGAAGAGGATCA; Oct4 R: AA-CACCTTTCCAAAGAGAACGCCC; Gata4 F: AGGGT-GAGCCTGTATGTAATGCCT; Gata4 R: AG-GACCTGCTGGCGTCTTAGATTT; Sox2 F: CACAT-GAAGGAGCACCCGGATTAT; Sox2 R: TCCGGGAAGCGTGTACTTATCCTT; Brachyury F: AGCTCTCCAACCTATGCGGACAAT; Brachyury R: TAT-CATGGGACTGCAGCATGGACA; Gata4 F: AGG GTGAGCCTG TAT GTA ATG C CT; Gata4 R: AGGACCTGC TGG CGT CTT AGAT TT; Notch2 F: TTCATGACATGCAGCCTTTGGCTC; Notch2 R: AG-GAACTGGATGTAACCTGCCCAA; Rex1 F: CTGGATTT-CAACTTGCGCACCCAT; Rex1 R: TTCAG-CATTTCTTCCCGGCCTTTG; β-actin F: GGAATCCTGTGGCATCCATGAAACTACA; and β-actin R: ACCAGACAGCACTGTGTTGGCATA.

Alkaline Phosphatase Assay. Cells were cultured at a density of 3×10^3 cells in 60 mm dishes for 120 and then were fixed with 4% paraformaldehyde for 2 min at room temperature. Alkaline phosphatase staining was performed using the SIGMAFAST Alkaline Phosphatase Substrate Tablets set (Sigma, St. Louis, MO, USA) following protocols provided by the manufacturer. Briefly, cells were incubated with p-nitrophenyl phosphate as an alkaline phosphatase substrate, and this produced a colorimetric reaction. Images were obtained using an Olympus IX71 microscope (Olympus, Hamburg, Germany), and they were processed with Adobe Photoshop (Adobe Systems Incorporated, San Jose, CA, USA) and quantified by ImageJ software.

Immunofluorescence Microscopy. R1/E cells (1.5 × 10^3) were fixed with 4% paraformaldehyde for 10 min, blocked for 30 min in phosphate-buffered saline (PBS) containing 3% BSA, and incubated overnight with anti-Nanog (Bethyl, Montgomery, TX, USA, BL1662). Detection of primary antibody was carried out with anti-rabbit-TRITC. Cells were counterstained with 300 nM DAPI. Fluorescence images were obtained using an Olympus IX71 microscope (Olympus, Hamburg, Germany) and a Leica DM 5500 microscope with a Leica DFC350FX CCD camera (Leica Microsystems, Wetzlar,

Germany). Images were processed with Adobe Photoshop (Adobe Systems Incorporated, San Jose, CA, USA).

Protein Extraction and Western Blotting. Cells were trypsinized from culture dishes, centrifuged at 1000 rpm for 5 min, and washed once with cold PBS. Proteins were extracted using 100 μL of RIPA buffer (Sigma, St. Louis, MO, USA) supplemented with protease inhibitor (Sigma, St. Louis, MO, USA) and phosphatase inhibitor cocktails (Sigma, St. Louis, MO, USA) for 45 min on ice and sonicated with three pulses for 10 s each at 10% amplitude in a Branson sonifier (Branson Ultrasonics Corporation, Danbury, CT, USA) to ensure high efficiency of lysis.

After centrifugation, the supernatant protein was quantified by Bradford assay. Protein extracts were denatured in Laemmli buffer containing 2.5% β-mercaptoethanol (Sigma) for 10 min at 98 °C. A total protein of 80 μg was separated using SDS-PAGE and transferred to the PVDF membrane. The membrane was probed with anti-Nanog (Bethyl, Montgomery, TX, USA, BL1662), anti-phospho (Thr172) and total AMPK (Cell Signaling Technology, Danvers, MA, USA), anti-GAPDH (Chemicon, Charlottesville, VA, USA), Phospho-GSK-3α/β (Ser21/9) and GSK-3β (Cell Signaling Technology, Danvers, MA, USA), and Anti-β-Actin (Sigma-Aldrich, St. Louis, USA).

This incubation was followed by incubation with their respective secondary peroxidase-conjugated antibodies. Immunoreactive bands were detected by chemiluminescence reagents (Millipore, Billerica, MA, USA) or Odyssey Infrared Technology (LI-COR, Lincoln, NE).

Cell Cycle Synchronization and Distribution by Flow Cytometry Analysis. Cells were treated with 2.5 mM thymidine for 12 h, washed with PBS, and incubated with 400 ng/mL nocodazole for 6 h. The numbers of synchronized cells in the G2/M phase at 0 time was analyzed, and >90% of cells were in this phase. Then, cells were washed with PBS. Thereafter, stem cells were treated with indicated stimuli for the time indicated. The treated cells were collected after trypsinization and washed with ice-cold PBS and fixed with 70% ethanol at −20 °C overnight. The following day, after cells had been washed with ice-cold PBS, they were incubated with 0.1% Triton X-100, propidium iodide (20 μg/mL), and RNase (200 μg/mL) for 15 min at room temperature in the dark. Data were collected from the flow cytometer (BD FACSCalibur; BD Biosciences) and analyzed with the accompanying software (CellQuest; BD Biosciences, San Diego, CA, USA). Ten thousand events per sample were counted, and the experiments were performed in triplicate. Data represent the mean ± standard deviations of three independent experiments.

shRNA-Induced Gene Silencing. For the generation of transfectants, mESCs were incubated with 9 μL of FuGENE HD transfection reagent (Roche Diagnostics, Mannheim, Germany) and 1 μg of DNA of five clones of MISSION shRNA AMPKα2 (Sigma, St. Louis, MO, USA) or MISSION pLKO.1-puro Control Vector (Sigma, St. Louis, MO, USA) in Opti-MEM medium for 3 h. Selection was initiated 24 h following transfection with 2 μg/mL puromycin (Sigma, St. Louis, MO, USA). Thereafter, cells were stimulated with the indicated treatments.

RNA Isolation, cDNA Synthesis, and Quantification of Gene Expression by RT-PCR. Collected ESCs were washed with PBS and then resuspended in Easy Blue reagent (Intron Biotechnology, Seoul, Korea) for RNA isolation. Following

phenol/chloroform extraction, total RNA was precipitated in 2-propanol, washed with ethanol, suspended in nuclease-free water and stored at −80 °C until being used for cDNA synthesis. The absorbance of the total RNA was evaluated at 260 and 280 nm to determine its concentration and purity using a NanoDrop ND-1000 Spectrophotometer (Nanodrop, Wilmington, DE, USA). Then, reverse transcription was performed with 1 μg of RNA using 5 U/μL MMLV Reverse Transcriptase (Promega, Madison, WI, USA) and 12.5 μg/mL random primers (Promega) in a volume of 25 μL and incubated for 1 h at 37 °C.

The cDNA obtained was diluted 1:10 and then used as a template for qRT-PCR using PerfeCTa SYBR GREEN Super Mix, Low ROX (Quanta Bioscience, Gaithersburg, MD, USA). Briefly, a 20 μL reaction included 10 μL of SYBR Green master mix 2X, 0.2 μM primers, 1 μL of diluted cDNA, and water. Data collection was at 60 °C for 1 min with the Applied Biosystems 7500 RT-PCR System (Applied Biosystems, Foster City, CA, USA). All the samples were normalized to the housekeeping gene β-actin, and all the data were analyzed with the DDCT method.

Statistical Analysis. The results are given as the mean ± standard error of the mean (SEM) of at least four independent experiments, except for the western blotting results, in which case a representative experiment is depicted in each figure. Comparisons between values were analyzed using one-way analysis of variance (ANOVA). Values were considered to be statistically significant when $p \leq 0.05$.

■ AUTHOR INFORMATION

Corresponding Author

　Gonzalo Alba − *Department of Medical Biochemistry and Molecular Biology, Universidad de Sevilla, Seville 41009, Spain;* ⬤ orcid.org/0000-0002-6598-2039; Phone: +34-955421044; Email: galbaj@us.es; Fax: +34-954907048

Authors

　Raquel Martínez − *Department of Regeneration and Cell Therapy, Andalusian Center for Molecular Biology and Regenerative Medicine-CABIMER, Universidad Pablo de Olavide-University of Seville-CSIC, Seville 41013, Spain*

　Fátima Postigo-Corrales − *Department of Regeneration and Cell Therapy, Andalusian Center for Molecular Biology and Regenerative Medicine-CABIMER, Universidad Pablo de Olavide-University of Seville-CSIC, Seville 41013, Spain*

　Soledad López − *Department of Medical Biochemistry and Molecular Biology, Universidad de Sevilla, Seville 41009, Spain*

　Consuelo Santa-María − *Department of Biochemistry and Molecular Biology, Universidad de Sevilla, Seville 41009, Spain*

　Juan Jiménez − *Department of Medical Biochemistry and Molecular Biology, Universidad de Sevilla, Seville 41009, Spain*

　Gladys M. Cahuana − *Department of Molecular Biology and Biochemical Engineering, Universidad Pablo de Olavide, Seville 41013, Spain; Biomedical Research Network for Diabetes and Related Metabolic Diseases-CIBERDEM, Instituto de Salud Carlos III, Madrid 28029, Spain*

　Bernat Soria − *Department of Regeneration and Cell Therapy, Andalusian Center for Molecular Biology and Regenerative Medicine-CABIMER, Universidad Pablo de Olavide-University of Seville-CSIC, Seville 41013, Spain; Biomedical Research Network for Diabetes and Related Metabolic Diseases-CIBERDEM, Instituto de Salud Carlos III, Madrid 28029, Spain; Cell Therapy Network, Madrid (RED-TERCEL),*

Instituto de Salud Carlos III, Madrid 28029, Spain; Universidad Miguel Hernández, Alicante 03550, Spain

　Francisco J. Bedoya − *Department of Regeneration and Cell Therapy, Andalusian Center for Molecular Biology and Regenerative Medicine-CABIMER, Universidad Pablo de Olavide-University of Seville-CSIC, Seville 41013, Spain; Department of Molecular Biology and Biochemical Engineering, Universidad Pablo de Olavide, Seville 41013, Spain; Biomedical Research Network for Diabetes and Related Metabolic Diseases-CIBERDEM, Instituto de Salud Carlos III, Madrid 28029, Spain; Cell Therapy Network, Madrid (RED-TERCEL), Instituto de Salud Carlos III, Madrid 28029, Spain*

　Juan R. Tejedo − *Department of Regeneration and Cell Therapy, Andalusian Center for Molecular Biology and Regenerative Medicine-CABIMER, Universidad Pablo de Olavide-University of Seville-CSIC, Seville 41013, Spain; Department of Molecular Biology and Biochemical Engineering, Universidad Pablo de Olavide, Seville 41013, Spain; Biomedical Research Network for Diabetes and Related Metabolic Diseases-CIBERDEM, Instituto de Salud Carlos III, Madrid 28029, Spain; Cell Therapy Network, Madrid (RED-TERCEL), Instituto de Salud Carlos III, Madrid 28029, Spain*

Complete contact information is available at:
https://pubs.acs.org/10.1021/acsomega.0c02137

Author Contributions

G.A., F.J.B., B.S., and J.R.T. conceived and designed the research. G.A., F.P.-C., and R.M. performed the experiments. G.A., C.S.-M., and J.R.T. analyzed the data. G.A., S.L., and G.M.C. performed data collection and preprocessing. G.A., C.S.-M., J.J., and J.R.T. wrote the paper.

Notes

The authors declare no competing financial interest.

■ ACKNOWLEDGMENTS

■ REFERENCES

(1) Brook, F. A.; Gardner, R. L. The Origin and Efficient Derivation of Embryonic Stem Cells in the Mouse. *Proc. Natl. Acad. Sci. U. S. A.* **1997**, *94*, 5709−5712.

(2) Evans, M. J.; Kaufman, M. H. Establishment in Culture of Pluripotential Cells from Mouse Embryos. *Nature* **1981**, *292*, 154−156.

(3) Martin, G. R. Isolation of a Pluripotent Cell Line from Early Mouse Embryos Cultured in Medium Conditioned by Teratocarcinoma Stem Cells. *Proc. Natl. Acad. Sci. U. S. A.* **1981**, *78*, 7634−7638.

(4) Chambers, I. The Molecular Basis of Pluripotency in Mouse Embryonic Stem Cells. *Cloning Stem Cells* **2004**, *6*, 386−391.

(5) Boiani, M.; Schöler, H. R. Regulatory Networks in Embryo-Derived Pluripotent Stem Cells. *Nat. Rev. Mol. Cell Biol.* **2005**, *6*, 872−881.

(6) Boeuf, H.; Hauss, C.; De Graeve, F.; Baran, N.; Kedinger, C. Leukemia Inhibitory Factor-Dependent Transcriptional Activation in Embryonic Stem Cells. *J. Cell Biol.* 1997, 138, 1207−1217.

(7) Loh, Y.-H.; Wu, Q.; Chew, J.-L.; Vega, V. B.; Zhang, W.; Chen, X.; Bourque, G.; George, J.; Leong, B.; Liu, J.; Wong, K.-Y.; Sung, K. W.; Lee, C. W. H.; Zhao, X.-D.; Chiu, K.-P.; Lipovich, L.; Kuznetsov, V. A.; Robson, P.; Stanton, L. W.; Wei, C.-L.; Ruan, Y.; Lim, B.; Ng, H.-H. The Oct4 and Nanog Transcription Network Regulates Pluripotency in Mouse Embryonic Stem Cells. *Nat. Genet.* 2006, 38, 431−440.

(8) Masui, S.; Ohtsuka, S.; Yagi, R.; Takahashi, K.; Ko, M. S.; Niwa, H. Rex1/Zfp42 Is Dispensable for Pluripotency in Mouse ES Cells. *BMC Dev. Biol.* 2008, 8, 45.

(9) Avilion, A. A.; Nicolis, S. K.; Pevny, L. H.; Perez, L.; Vivian, N.; Lovell-Badge, R. Multipotent Cell Lineages in Early Mouse Development Depend on SOX_2 Function. *Genes Dev.* 2003, 17, 126−140.

(10) Miyamoto, T.; Furusawa, C.; Kaneko, K. Pluripotency, Differentiation, and Reprogramming: A Gene Expression Dynamics Model with Epigenetic Feedback Regulation. *PLoS Comput. Biol.* 2015, 11, No. e1004476.

(11) Bernardo, A. S.; Faial, T.; Gardner, L.; Niakan, K. K.; Ortmann, D.; Senner, C. E.; Callery, E. M.; Trotter, M. W.; Hemberger, M.; Smith, J. C.; Bardwell, L.; Moffett, A.; Pedersen, R. A. BRACHYURY and CDX2 Mediate BMP-Induced Differentiation of Human and Mouse Pluripotent Stem Cells into Embryonic and Extraembryonic Lineages. *Cell Stem Cell* 2011, 9, 144−155.

(12) Lewis, K. L.; Caton, M. L.; Bogunovic, M.; Greter, M.; Grajkowska, L. T.; Ng, D.; Klinakis, A.; Charo, I. F.; Jung, S.; Gommerman, J. L.; Ivanov, I. I.; Liu, K.; Merad, M.; Reizis, B. Notch2 Receptor Signaling Controls Functional Differentiation of Dendritic Cells in the Spleen and Intestine. *Immunity* 2011, 35, 780−791.

(13) Li, W.-Z.; Ai, Z.-Y.; Wang, Z.-W.; Chen, L.-L.; Guo, Z.-K.; Zhang, Y. GATA-1 Directly Regulates Nanog in Mouse Embryonic Stem Cells. *Biochem. Biophys. Res. Commun.* 2015, 465, 575−579.

(14) Chen, L.; Yang, M.; Dawes, J.; Khillan, J. S. Suppression of ES Cell Differentiation by Retinol (Vitamin A) via the Overexpression of Nanog. *Differentiation* 2007, 75, 682−693.

(15) Chambers, I.; Colby, D.; Robertson, M.; Nichols, J.; Lee, S.; Tweedie, S.; Smith, A. Functional Expression Cloning of Nanog, a Pluripotency Sustaining Factor in Embryonic Stem Cells. *Cell* 2003, 113, 643−655.

(16) Filipczyk, A.; Marr, C.; Hastreiter, S.; Feigelman, J.; Schwarzfischer, M.; Hoppe, P. S.; Loeffler, D.; Kokkaliaris, K. D.; Endele, M.; Schauberger, B.; Hilsenbeck, O.; Skylaki, S.; Hasenauer, J.; Anastassiadis, K.; Theis, F. J.; Schroeder, T. Network Plasticity of Pluripotency Transcription Factors in Embryonic Stem Cells. *Nat. Cell Biol.* 2015, 17, 1235−1246.

(17) Pan, G. J.; Chang, Z. Y.; Schöler, H. R.; Pei, D. Stem Cell Pluripotency and Transcription Factor Oct4. *Cell Res.* 2002, 12, 321−329.

(18) Shi, W.; Wang, H.; Pan, G.; Geng, Y.; Guo, Y.; Pei, D. Regulation of the Pluripotency Marker *Rex-1* by Nanog and Sox2. *J. Biol. Chem.* 2006, 281, 23319−23325.

(19) Grigorash, B. B.; Suvorova, I. I.; Pospelov, V. A. AICAR-Dependent Activation of AMPK Kinase Is Not Accompanied by G1/S Block in Mouse Embryonic Stem Cells. *Mol. Biol.* 2018, 52, 419−429.

(20) Folmes, C. D. L.; Dzeja, P. P.; Nelson, T. J.; Terzic, A. Metabolic Plasticity in Stem Cell Homeostasis and Differentiation. *Cell Stem Cell* 2012, 11, 596−606.

(21) Adamo, L.; Zhang, Y.; García-Cardeña, G. AICAR Activates the Pluripotency Transcriptional Network in Embryonic Stem Cells and Induces KLF4 and KLF2 Expression in Fibroblasts. *BMC Pharmacol.* 2009, 9, 2.

(22) Lees, J. G.; Gardner, D. K.; Harvey, A. J. Pluripotent Stem Cell Metabolism and Mitochondria: Beyond ATP. *Stem Cells Int.* 2017, 2017, 1−17.

(23) Paling, N. R. D.; Wheadon, H.; Bone, H. K.; Welham, M. J. Regulation of Embryonic Stem Cell Self-Renewal by Phosphoinositide

3-Kinase-Dependent Signaling. *J. Biol. Chem.* 2004, 279, 48063−48070.

(24) Storm, M. P.; Bone, H. K.; Beck, C. G.; Bourillot, P.-Y.; Schreiber, V.; Damiano, T.; Nelson, A.; Savatier, P.; Welham, M. J. Regulation of Nanog Expression by Phosphoinositide 3-Kinase-Dependent Signaling in Murine Embryonic Stem Cells. *J. Biol. Chem.* 2007, 282, 6265−6273.

(25) Storm, M. P.; Kumpfmueller, B.; Thompson, B.; Kolde, R.; Vilo, J.; Hummel, O.; Schulz, H.; Welham, M. J. Characterization of the Phosphoinositide 3-Kinase-Dependent Transcriptome in Murine Embryonic Stem Cells: Identification of Novel Regulators of Pluripotency. *Stem Cells* 2009, 27, 764−775.

(26) Forde, J. E.; Dale, T. C. Glycogen Synthase Kinase 3: A Key Regulator of Cellular Fate. *Cell. Mol. Life Sci.* 2007, 64, 1930−1944.

(27) Sanchez-Ripoll, Y.; Bone, H. K.; Owen, T.; Guedes, A. M. V.; Abranches, E.; Kumpfmueller, B.; Spriggs, R. V.; Henrique, D.; Welham, M. J. Glycogen Synthase Kinase-3 Inhibition Enhances Translation of Pluripotency-Associated Transcription Factors to Contribute to Maintenance of Mouse Embryonic Stem Cell Self-Renewal. *PLoS One* 2013, 8, No. e60148.

(28) Tejedo, J. R.; Tapia-Limonchi, R.; Mora-Castilla, S.; Cahuana, G. M.; Hmadcha, A.; Martin, F.; Bedoya, F. J.; Soria, B. Low Concentrations of Nitric Oxide Delay the Differentiation of Embryonic Stem Cells and Promote Their Survival. *Cell Death Dis.* 2010, 1, e80−e80.

(29) Tapia-Limonchi, R.; Cahuana, G. M.; Caballano-Infantes, E.; Salguero-Aranda, C.; Beltran-Povea, A.; Hitos, A. B.; Hmadcha, A.; Martin, F.; Soria, B.; Bedoya, F. J.; Tejedo, J. R. Nitric Oxide Prevents Mouse Embryonic Stem Cell Differentiation Through Regulation of Gene Expression, Cell Signaling, and Control of Cell Proliferation. *J. Cell. Biochem.* 2016, 117, 2078−2088.

(30) Štefková, K.; Procházková, J.; Pacherník, J. Alkaline Phosphatase in Stem Cells. *Stem Cells Int.* 2015, 1.

(31) Liang, X.; Wang, P.; Gao, Q.; Tao, X. Exogenous Activation of LKB1/AMPK Signaling Induces G_1 Arrest in Cells with Endogenous LKB1 Expression. *Mol. Med. Rep.* 2014, 9, 1019−1024.

(32) Theka, I.; Sottile, F.; Cammisa, M.; Bonnin, S.; Sanchez-Delgado, M.; Di Vicino, U.; Neguembor, M. V.; Arumugam, K.; Aulicino, F.; Monk, D.; Riccio, A.; Cosma, M. P. Wnt/β-Catenin Signaling Pathway Safeguards Epigenetic Stability and Homeostasis of Mouse Embryonic Stem Cells. *Sci. Rep.* 2019, 9, 948.

(33) Shi, X.; Wu, Y.; Ai, Z.; Liu, X.; Yang, L.; Du, J.; Shao, J.; Guo, Z.; Zhang, Y. AICAR Sustains J1 Mouse Embryonic Stem Cell Self-Renewal and Pluripotency by Regulating Transcription Factor and Epigenetic Modulator Expression. *Cell. Physiol. Biochem.* 2013, 32, 459−475.

(34) Chae, H.-D.; Lee, M.-R.; Broxmeyer, H. E. 5-Aminoimidazole-4-Carboxyamide Ribonucleoside Induces G(1)/S Arrest and Nanog Downregulation via P53 and Enhances Erythroid Differentiation. *Stem Cells* 2012, 30, 140−149.

(35) Wang, J.; Alexander, P.; McKnight, S. L. Metabolic Specialization of Mouse Embryonic Stem Cells. *Cold Spring Harbor Symp. Quant. Biol.* 2011, 76, 183−193.

(36) Shi, X.; YongyanWu; Ai, Z.; Du, J.; Cao, L.; Guo, Z.; Zhang, Y. MicroRNA Modulation Induced by AICA Ribonucleotide in J1 Mouse ES Cells. *PLoS One* 2014, 9, No. e103724.

(37) Shen, C.; Ka, S.-O.; Kim, S. J.; Kim, J. H.; Park, B.-H.; Park, J. H. Metformin and AICAR Regulate NANOG Expression via the JNK Pathway in HepG2 Cells Independently of AMPK. *Tumor Biol.* 2016, 37, 11199−11208.

(38) Andäng, M.; Hjerling-Leffler, J.; Moliner, A.; Lundgren, T. K.; Castelo-Branco, G.; Nanou, E.; Pozas, E.; Bryja, V.; Halliez, S.; Nishimaru, H.; Wilbertz, J.; Arenas, E.; Koltzenburg, M.; Charnay, P.; El Manira, A.; Ibañez, C. F.; Ernfors, P. Histone H2AX-Dependent GABA(A) Receptor Regulation of Stem Cell Proliferation. *Nature* 2008, 451, 460−464.

(39) Liu, X.; Chhipa, R. R.; Nakano, I.; Dasgupta, B. The AMPK Inhibitor Compound C Is a Potent AMPK-Independent Antiglioma Agent. *Mol. Cancer Ther.* 2014, 13, 596−605.

(40) Suvorova, I. I.; Knyazeva, A. R.; Petukhov, A. V.; Aksenov, N. D.; Pospelov, V. A. Resveratrol Enhances Pluripotency of Mouse Embryonic Stem Cells by Activating AMPK/Ulk1 Pathway. *Cell Death Discov.* **2019**, *5*, 61.

(41) Lin, C.-Y.; Chin, Y.-T.; Kuo, P.-J.; Lee, H.-W.; Huang, H.-M.; Lin, H.-Y.; Weng, I.-T.; Hsiung, C.-N.; Chan, Y.-H.; Lee, S.-Y. 2,3,5,4′-Tetrahydroxystilbene-2-O-β-Glucoside Potentiates Self-Renewal of Human Dental Pulp Stem Cells via the AMPK/ERK/SIRT1 Axis. *Int. Endod. J.* **2018**, *51*, 1159−1170.

(42) Gong, J.; Gu, H.; Zhao, L.; Wang, L.; Liu, P.; Wang, F.; Xu, H.; Zhao, T. Phosphorylation of ULK1 by AMPK Is Essential for Mouse Embryonic Stem Cell Self-Renewal and Pluripotency. *Cell Death Dis.* **2018**, *9*, 38.

(43) Ruvolo, P. P.; Qiu, Y.; Coombes, K. R.; Zhang, N.; Neeley, E. S.; Ruvolo, V. R.; Hail, N., Jr.; Borthakur, G.; Konopleva, M.; Andreeff, M.; Kornblau, S. M. Phosphorylation of GSK3α/β Correlates with Activation of AKT and Is Prognostic for Poor Overall Survival in Acute Myeloid Leukemia Patients. *BBA Clin.* **2015**, *4*, 59−68.

(44) MacDonald, B. T.; Tamai, K.; He, X. Wnt/β-Catenin Signaling: Components, Mechanisms, and Diseases. *Dev. Cell* **2009**, *17*, 9−26.

(45) Doble, B. W.; Patel, S.; Wood, G. A.; Kockeritz, L. K.; Woodgett, J. R. Functional Redundancy of GSK-3α and GSK-3β in Wnt/β-Catenin Signaling Shown by Using an Allelic Series of Embryonic Stem Cell Lines. *Dev. Cell* **2007**, *12*, 957−971.

(46) Raggioli, A.; Junghans, D.; Rudloff, S.; Kemler, R. Beta-Catenin Is Vital for the Integrity of Mouse Embryonic Stem Cells. *PLoS One* **2014**, *9*, No. e86691.

(47) Kelly, K. F.; Ng, D. Y.; Jayakumaran, G.; Wood, G. A.; Koide, H.; Doble, B. W. β-Catenin Enhances Oct-4 Activity and Reinforces Pluripotency through a TCF-Independent Mechanism. *Cell Stem Cell* **2011**, *8*, 214−227.

(48) Roccio, M.; Schmitter, D.; Knobloch, M.; Okawa, Y.; Sage, D.; Lutolf, M. P. Predicting Stem Cell Fate Changes by Differential Cell Cycle Progression Patterns. *Development* **2013**, *140*, 459−470.

(49) Coronado, D.; Godet, M.; Bourillot, P.-Y.; Tapponnier, Y.; Bernat, A.; Petit, M.; Afanassieff, M.; Markossian, S.; Malashicheva, A.; Iacone, R.; Anastassiadis, K.; Savatier, P. A Short G1 Phase Is an Intrinsic Determinant of Naïve Embryonic Stem Cell Pluripotency. *Stem Cell Res.* **2013**, *10*, 118−131.

(50) Gonzales, K. A. U.; Liang, H.; Lim, Y.-S.; Chan, Y.-S.; Yeo, J.-C.; Tan, C.-P.; Gao, B.; Le, B.; Tan, Z.-Y.; Low, K.-Y.; Liou, Y.-C.; Bard, F.; Ng, H.-H. Deterministic Restriction on Pluripotent State Dissolution by Cell-Cycle Pathways. *Cell* **2015**, *162*, 564−579.

(51) Waisman, A.; Sevlever, F.; Costa, M. E.; Cosentino, M. S.; Miriuka, S. G.; Ventura, A. C.; Guberman, A. S. Cell Cycle Dynamics of Mouse Embryonic Stem Cells in the Ground State and during Transition to Formative Pluripotency. *Sci. Rep.* **2019**, *9*, 8051.

(52) Cannon, D.; Corrigan, A. M.; Miermont, A.; McDonel, P.; Chubb, J. R. Multiple Cell and Population-Level Interactions with Mouse Embryonic Stem Cell Heterogeneity. *Development* **2015**, *142*, 2840−2849.

(53) Sineva, G. S.; Pospelov, V. A. Inhibition of GSK3β Enhances Both Adhesive and Signalling Activities of β-Catenin in Mouse Embryonic Stem Cells. *Biol. Cell* **2010**, *102*, 549.

(54) Zang, Y.; Yu, L.-F.; Pang, T.; Fang, L.-P.; Feng, X.; Wen, T.-Q.; Nan, F.-J.; Feng, L.-Y.; Li, J. AICAR Induces Astroglial Differentiation of Neural Stem Cells via Activating the JAK/STAT3 Pathway Independently of AMP-Activated Protein Kinase. *J. Biol. Chem.* **2008**, *283*, 6201−6208.